Polymer 50 (2009) 1901–1907

Contents lists available at ScienceDirect

Polymer

journal homepage: www.elsevier.com/locate/polymer

Polymorphism of syndiotactic poly(*p*-fluoro-styrene)

Nunzia Galdi*, Alexandra R. Albunia, Leone Oliva, Gaetano Guerra

Università degli Studi di Salerno, Chemistry Department and INSTM Research Unit, Via Ponte don Melillo, 84084 Fisciano, Italy

ARTICLE INFO

Article history:
Received 29 September 2008
Received in revised form
10 February 2009
Accepted 10 February 2009
Available online 21 February 2009

Keywords:
Polymer science
Polymer synthesis
Polymer physical chemistry

ABSTRACT

Syndiotactic poly(*p*-fluoro-styrene) (s-PPFS) has been prepared with a polymerization procedure which allows reaching high average molecular masses and satisfactory yields. The polymorphic behavior of the polymer has been mainly studied by X-ray diffraction, calorimetric and infrared analyses. The main crystalline phase of s-PPFS, obtained by melt processing or cold-crystallization, exhibits *trans*-planar chains, is orthorhombic ($a = 9.5$ Å, $b = 28.7$ Å, $c = 5.1$ Å) and melts at nearly 320 °C. The X-ray analysis shows a strict analogy of this orthorhombic phase with the β phase of s-PS, also as for the occurrence of two limit ordered (β″) and disordered (β′) modifications, which differ for the intensity of reflections characterized by $h + k = 2n + 1$. A metastable crystalline phase, also exhibiting *trans*-planar chains, has been observed for as-polymerized samples as well as for amorphous samples crystallized by sorption of toluene or 1,4-difluoro-benzene. Mainly on the basis of solvent sorption and desorption experiments, it is suggested that this metastable phase is a co-crystalline phase with the low-molecular-mass guest molecules.

1. Introduction

The syndiospecific polymerization of styrene monomers [1–4] has provided in the two last decades several new syndiotactic polymers, like e.g. polystyrene (s-PS) [5–9], poly(*p*-methyl-styrene) (s-PPMS) [10–13], poly(*p*-*n*-butyl-styrene) [14], poly(*p*-chloro-styrene) (s-PPCS) [15] and poly(*m*-methyl-styrene) (s-PMMS) [16,17] generally presenting very complex polymorphic behaviors.

Most of these syndiotactic polymers (s-PS [18–26], s-PPMS [27–33], s-PPCS [15], s-PMMS [16,17]) are also able to form co-crystalline phases with low-molecular-mass molecules. Moreover, s-PS by suitable procedures of guest removal is able to form two different nanoporous crystalline phases (named δ [34–38] and ε [39,40]), which present their nanoporosity organized as cavities and channels, respectively.

Recent studies have shown that polymer co-crystals reducing guest diffusivity [41–44] and imposing guest orientational order [45–49], can be used as advanced materials mainly for optical applications (e.g. chromophore [50], fluorescent [51,52] and non-linear optical [53] and photo-reactive [54,55] materials). Moreover, nanoporous crystalline phases are suitable for applications in chemical separations and air/water purification [56–62] as well as in sensorics [63–68].

Syndiotactic poly(*p*-fluoro-styrene) (s-PPFS) has been synthesized several years ago but only a very limited information (a ^{13}C NMR spectrum and numerical values for the glass transition and the melting temperature) have been reported [2,4]. In the present paper we describe a slightly modified synthetic procedure, which allows reaching definitely larger conversions. Most of the paper is, however, devoted to the study of the polymorphic behavior of s-PPFS, mainly by X-ray diffraction, infrared and calorimetric analyses. The collected X-ray data have also allowed establishing that the main crystalline structure of s-PPFS is similar to the β crystalline structure of s-PS [69,70].

2. Experimental part

2.1. Materials

Pentamethylcyclopentadienyl titanium trichloride (Cp^*TiCl_3) and *p*-fluoro-styrene are commercially available (Aldrich) and were used without further purification. The methylalumoxane (MAO) was dried from the commercial 10% toluene solution (Witco) by removing solvent and traces of trimethyl aluminum under reduced pressure. The toluene before the use was kept under reflux in the presence of sodium for 48 h, and then distilled under nitrogen atmosphere.

* Corresponding author. Tel.: +39 89969362; fax: +39 89969603.
E-mail address: gnunzia@unisa.it (N. Galdi).

0032-3861/$ – see front matter © 2009 Elsevier Ltd. All rights reserved.
doi:10.1016/j.polymer.2009.02.015

2.2. Polymerization procedure

In a 100 ml round bottom flask were introduced under nitrogen atmosphere 7 ml of toluene, 6 ml of *p*-fluoro-styrene and 1.0 g of dry MAO. The homogeneous mixture was thermostated at 50 °C and kept under magnetic stirring for 10 min, then the catalyst (Cp^*TiCl_3 5.0 mg) was added (Al/Ti molar ratio = 1000). After 100 h the polymerization mixture was poured into acidified ethanol, the polymer recovered through filtration, washed two times with fresh ethanol, and then dried in vacuum at 50 °C for 2 h. Yield 1.5 g.

2.3. ^{13}C NMR analysis

The spectrum was recorded on an AM 250 Bruker spectrometer operating at 62.89 MHz in the Fourier transform mode and at the temperature of 383 K. The sample was prepared by dissolving 30 mg of polymer into 0.5 ml of tetrachloro-1,2-dideuterioethane. The chemical shifts are referred to the central peak of $C_2D_2Cl_4$ used as internal reference at $\delta = 74.26$ ppm.

2.4. GPC analysis

The analysis of the polymer was performed at 135 °C by Waters instrument GPCV 2000 equipped with refractive index and viscosimeter detectors, using four PSS columns set consisting of, 10^5, 10^4, 10^3 and 10^2 Å (pore size) and 10 μm (particle size). *o*-Dichlorobenzene was the carrier solvent used with a flow rate of 1.0 ml/min. The calibration curve was established with polystyrene standards.

2.5. Thermogravimetric analysis

Thermogravimetric analyses (TGA) were carried out by a Mettler TG50 thermobalance in a flowing nitrogen atmosphere at a heating rate of 10 °C/min.

2.6. Wide-angle X-ray diffraction

Wide-angle X-ray diffraction patterns with nickel filtered CuKα radiation were obtained, in reflection, with an automatic Bruker diffractometer.

2.7. Fourier transform infrared spectra

Infrared spectra were obtained at a resolution of 2.0 cm^{-1} with a Vertex 70 Bruker spectrometer equipped with deuterated triglycine sulphate (DTGS) detector and a KBr beam splitter. The frequency scale was internally calibrated to 0.01 cm^{-1} using a He–Ne laser. 32 scans were signal averaged to reduce the noise.

2.8. Differential scanning calorimetry

Differential scanning calorimetry (DSC) measurements were carried out with a DSC 2920 TA Instruments in a flowing nitrogen atmosphere, at heating rate of 10 °C/min and 20 °C/min.

3. Results and discussion

3.1. Synthesis of s-PPFS

The synthetic route we chose for the *p*-fluoro-styrene syndiospecific polymerization is a modification of what Ishihara et al. reported [3]. In order to improve the very low reported monomer conversion (<1%), pentamethylcyclopentadienyl titanium trichloride (Cp^*TiCl_3) activated by methylalumoxane (MAO) was employed as catalyst, and the polymerization mixture was kept reacting for several days at 50 °C. In this manner syndiotactic poly-*p*-fluoro-styrene was obtained in reasonable yield (about 20%).

The amount of stereo-defects was evaluated from the ^{13}C NMR spectrum (Fig. 1), where the signals of stereo-irregular tetrads can be expected, in the methylene region, between 46.5 and 45.6 ppm and between 44.3 and 42.6 ppm (TMS scale), in accordance with what reported for the syndiotactic polystyrene [2]. In this manner a value of 0.92 of the probability of syndiotactic enchainment P_r was determined. This corresponds to a syndiotacticity, expressed in terms of racemic rrrr pentads of 72%, i.e. very close to the value reported in the patent literature (70%) [2].

The weight-average molecular mass obtained by GPC is $M_w = 1.0 \times 10^5$, i.e. definitely higher than that one reported in literature for the sample obtained by using cyclopentadienyltitanium trichloride ($M_w = 0.29 \times 10^5$) [2], while the polydispersity index, $M_w/M_n = 2.5$, is typical of polymers obtained through single site catalyst.

3.2. Crystallization, crystal-to-crystal transitions and melting of s-PPFS

The X-ray diffraction pattern of an s-PPFS sample, as obtained by the described polymerization procedure, is reported in Fig. 2a. The presence of at least four diffraction peaks (for $d = 9.41$ nm, 7.25 nm, 6.46 nm, 4.85 nm, corresponding to $2\theta_{CuK\alpha} = 9.4°, 12.2°, 13.7°, 18.3°$) clearly indicates the formation of a crystalline phase. TGA analyses, shown in Fig. 3a, indicate that as-polymerized samples, although washed with ethanol and dried in vacuum at 50 °C, include nearly 3.5 wt% of low-molecular-mass compounds (mostly toluene).

All procedures leading to the residual toluene removal, like e.g. extractions by acetonitrile or acetone at room temperature or by supercritical carbon dioxide as well as by annealing above 80 °C (i.e. close to the polymer glass transition temperature) as well as long term storage at room temperature (e.g. one year), produce a similar and irreversible change in the X-ray diffraction pattern. Just as an example, the X-ray diffraction pattern of the as-polymerized s-PPFS sample, after complete extraction of low-molecular-mass compounds by CO_2 pressure of 200 bars at 40 °C, is shown in Fig. 2b. This pattern shows that the two peaks occurring, for the as-polymerized sample at $2\theta_{CuK\alpha} = 9.4°$, 13.7° are shifted by the solvent removal in opposite directions $2\theta_{CuK\alpha} = 9.6°$, 13.4°, thus indicating the formation of a different unit cell while the degree of crystallinity remains low.

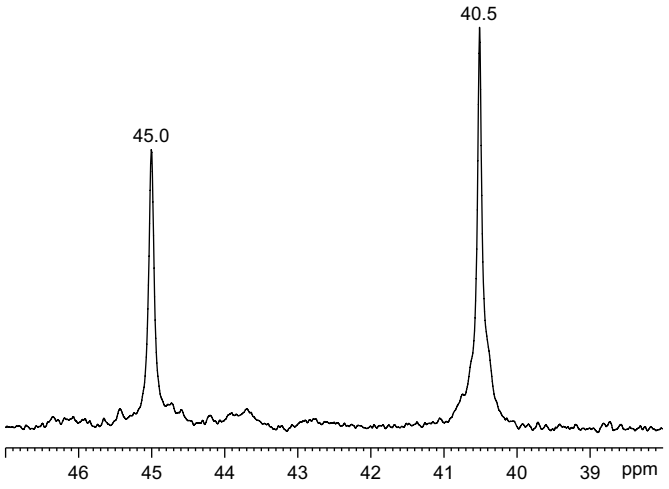

Fig. 1. Aliphatic region of the ^{13}C NMR spectrum of s-PPFS as obtained by polymerization with the catalytic system Cp^*TiCl_3/MAO.

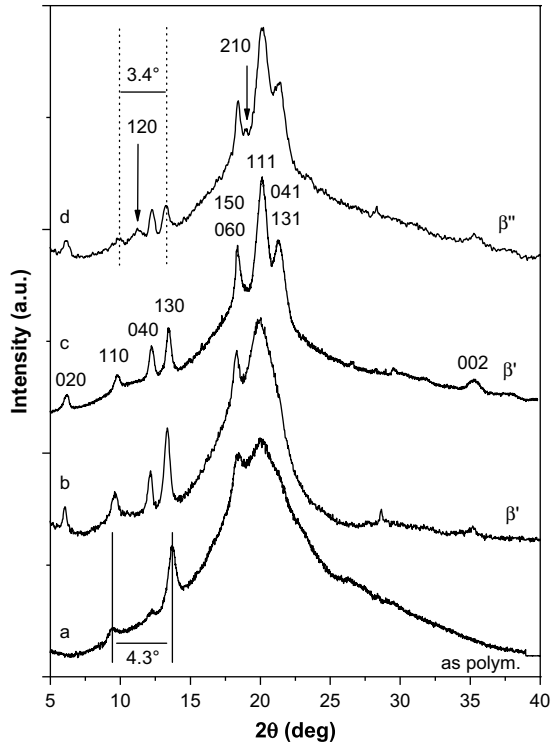

Fig. 2. X-ray diffraction patterns (CuKα) of s-PPFS powder samples: (a) as-polymerized; (b) after extraction of low-molecular-mass compounds by supercritical CO_2; (c) after annealing at 270 °C; (d) after annealing at 310 °C.

This new crystalline phase can be easily perfected by high-temperature annealing, as shown by the X-ray diffraction pattern of the as-polymerized sample after annealing at 270 °C (Fig. 2c) and at 310 °C (Fig. 2d). The $2\theta_{CuK\alpha}$ and Bragg distances corresponding to the observed peaks are listed in the first two column of Table 1. It is worth noting that by the high-temperature annealing (in the range 300–320 °C, i.e. close to the polymer melting temperature) the two above cited diffraction peaks become further close ($2\theta_{CuK\alpha} = 9.8°$, 13.1°). Hence, the distance between the observed peaks is 4.3° for the native crystalline phase (Fig. 2a) while is 3.4° for the high-temperature annealed phase (Fig. 2d). It is also worth noting that, by the high-temperature annealing, two minor peaks (indicated by arrows in Fig. 2d and by asterisks in Table 1) clearly appear.

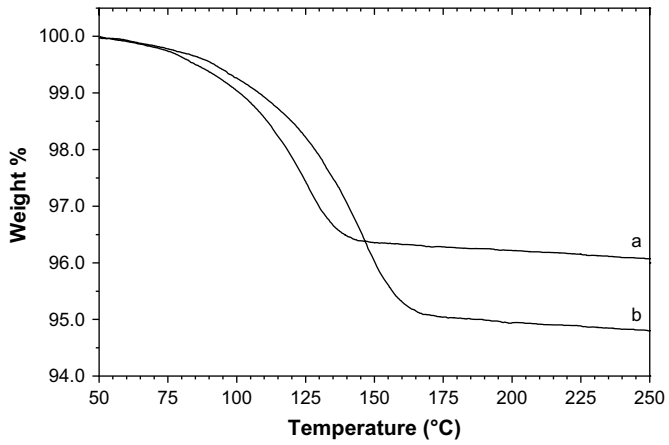

Fig. 3. Thermogravimetric analysis of s-PPFS samples desiccated in vacuum at 50 °C: (a) as-polymerized, (b) after crystallization of an amorphous sample by *p*-di-fluoro-benzene sorption.

Table 1
Diffraction angles (for CuKα radiation) and Bragg distances, as observed for the X-ray diffraction pattern of the s-PPFS annealed at 310 °C (Fig. 2d). *h*, *k*, *l* and d_{calc} are the Miller indexes and the calculated Bragg distances corresponding to an orthorhombic unit cell with $a = 9.5$ Å, $b = 28.7$ Å, $c = 5.1$ Å.

$2\theta_{obs}$	d_{obs}	*h*	*k*	*l*	d_{calc}
6.15	14.37	0	2	0	14.35
9.8	9.02	1	1	0	9.02
11.2*	7.90	1	2	0	7.92
12.25	7.22	0	4	0	7.18
13.1	6.76	1	3	0	6.74
18.4	4.82	1	5	0	4.91
		0	6	0	4.78
19.0*	4.67	2	1	0	4.68
20.1	4.42	1	1	1	4.44
21.3	4.17	2	3	0	4.25
		0	4	1	4.16
		1	3	1	4.07
26.5	3.36	2	6	0	3.37
29.5	3.03				
30.5	2.93	3	4	0	2.90
32	2.80	1	10	0	2.75
35.2	2.55	0	0	2	2.55
37.8	2.38	0	4	2	2.41
		1	3	2	2.39

A fully amorphous sample (Fig. 4a) can be obtained by melting above 330 °C followed by quenching in water and ice. The availability of the X-ray diffraction pattern of a fully amorphous sample allows an easy determination of the degree of crystallinity of the samples of Fig. 2a–d, which is close to 10%, 16%, 26% and 28%, respectively.

The degree of crystallinity of the s-PPFS samples, independent of the crystallization procedure and also after extensive annealing, remains always lower than 30%. This is consistent with the syndiotacticity degree being definitely

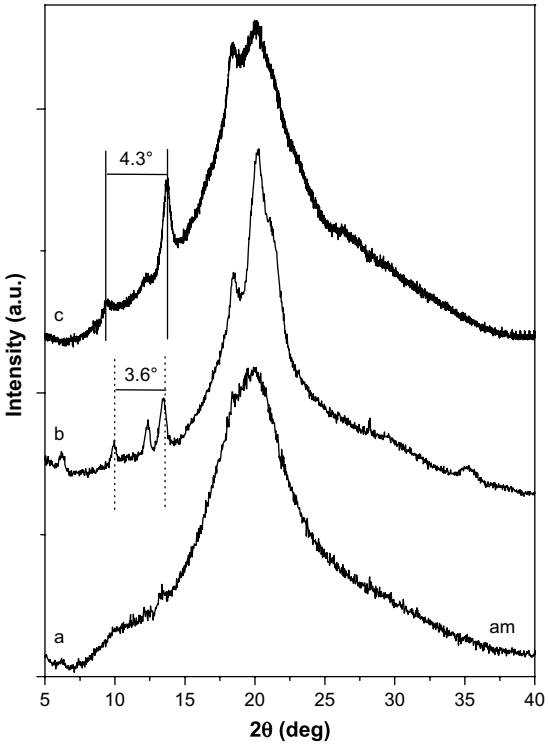

Fig. 4. X-ray diffraction patterns (CuKα) of s-PPFS samples: (a) quenched amorphous; (b) crystallized by chloroform sorption; (c) crystallized by *p*-di-fluoro-benzene sorption.

lower than for other syndiotactic polystyrenes (see, e.g. Table 4 of Ref. [2]).

Thermal annealing procedures on this amorphous sample lead to the formation of crystalline phases analogous to those shown in Fig. 2b–d. Amorphous s-PS samples can also be crystallized by solvent sorption. In particular, most solvents induce the same crystalline phase obtained by thermal treatments crystallization (Fig. 2b). Just an example, the X-ray diffraction pattern of a sample crystallized by chloroform sorption (at room temperature for 72 h) is shown in Fig. 4b.

Only for the case of crystallization induced by *p*-di-fluoro-benzene (Fig. 4c), a crystalline phase similar to the native crystalline phase of the as-polymerized sample (Fig. 2a) has been obtained. The similarity extends also to other relevant features: (i) the inclusion of a large amount of residual solvent, also after desiccation in vacuum at 50 °C (nearly 5% after desiccation at 35 °C under vacuum, as shown by the TGA analysis of Fig. 3b); (ii) the irreversible change into the thermodynamically stable crystalline phase (of Fig. 2b–d and Table 1), by any procedure leading to solvent removal.

These results suggest that the metastable crystalline phases of Figs. 2 and 4c, could be co-crystalline phases, including toluene and *p*-di-fluoro-benzene, respectively.

The DSC scans for the heating rate of 10 °C/min, of the as-polymerized, desiccated and annealed samples of Fig. 2a–d are reported in Fig. 5a–d, respectively.

The scan of Fig. 5a, besides the glass transition and the endothermic peak due to the toluene guest evaporation (in the range 80–120 °C) and minor peaks in the range 230–290 °C, shows a narrow melting peak at 321 °C. Simpler is the DSC scan of the as-polymerized samples after complete toluene removal (Fig. 5b), clearly showing, beside the melting temperature, a well defined glass transition at nearly 110 °C.

In this respect it is worth noting that the reported T_g values, as obtained by the same DSC technique, are nearly 130, 110 and 100 °C for s-PPCS [15], s-PPMS [30] and s-PS [71,72], respectively. Hence, as reasonably expected on the basis of the bulkiness of the phenyl ring substituents, the T_g of s-PPFS is similar to that one of s-PPMS and intermediate between those of s-PPCS and s-PS. The definitely lower T_g value reported for s-PPFS in Ref. [4] (94 °C) could be possibly due to the presence of some residual solvent molecules.

The observed T_m value, on the other hand, is very close to that one reported in Ref. [4] (322 °C) and also close to that one observed for s-PPCS (324 °C) [15] while larger than those observed for the highest melting crystalline phase of s-PPMS (form III, 224 °C) [10] and s-PS (≈270 °C) [5–9]. It is also worth adding that the observed T_m value is only slightly increased, because of re-crystallization phenomena occurring during the DSC scan. In fact, the melting temperature of the as-polymerized and desiccated samples of Fig. 2a and b is only slightly decreased when the DSC scans are conducted at higher heating rates (e.g. 318 °C for h.r. = 20 °C/min).

The DSC scans of the annealed samples (Fig. 5c and d) show the presence of broad melting peaks in the range 280–320 °C, whose position and shape strongly depend on the annealing conditions and heating rate, together with a broad glass transition located in the range 70–100 °C. The large decreases of T_g and T_m with respect to the scans of the unannealed samples (Fig. 5a and b) clearly indicate the occurrence of some polymer degradation for annealing temperatures higher than 270 °C.

The scan of the fully amorphous sample, whose X-ray diffraction pattern is shown in Fig. 4a (Fig. 5e) presents well defined glass transition (≈85 °C) crystallization (≈130 °C) and melting (310 °C) temperatures, which are also substantially decreased by partial polymer degradation associated with the melting at 330 °C.

3.3. Crystal structure of the thermally stable s-PPFS phase (β phase and β′,β″ modifications)

The Bragg distances collected in Table 1 can be easily indexed by an orthorhombic unit cell with $a = 9.5$ Å, $b = 28.7$ Å, $c = 5.1$ Å,

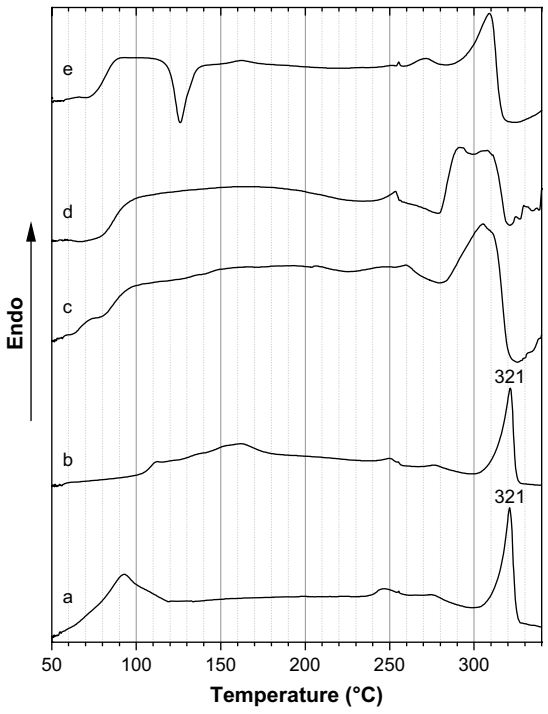

Fig. 5. DSC scans, for the heating rate of 10 K/min, of s-PPFS samples: (a) as-polymerized; (b) desiccated by CO_2; (c) annealed at 270 °C (β′); (d) annealed at 310 °C (β″); (e) amorphous as obtained by melt quenching.

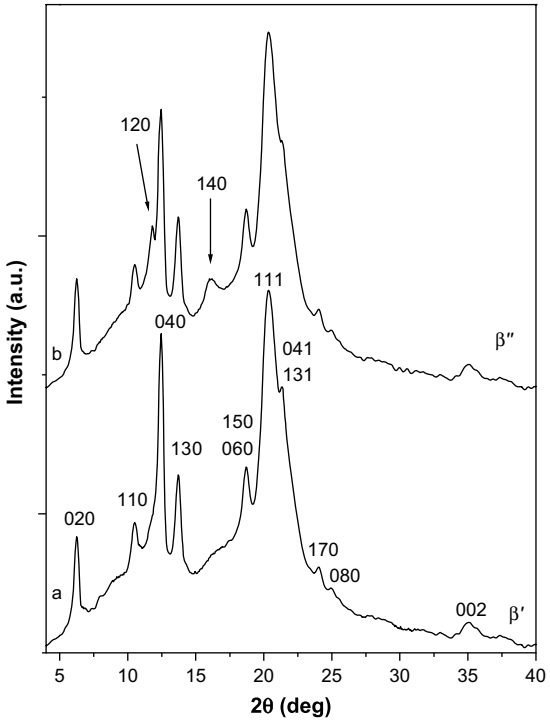

Fig. 6. X-ray diffraction patterns (CuKα) of unoriented s-PS samples, exhibiting the disordered β′ (a) and ordered β″ modifications (b). Close to the main peaks the Miller indexes of the contributing reflections are indicated.

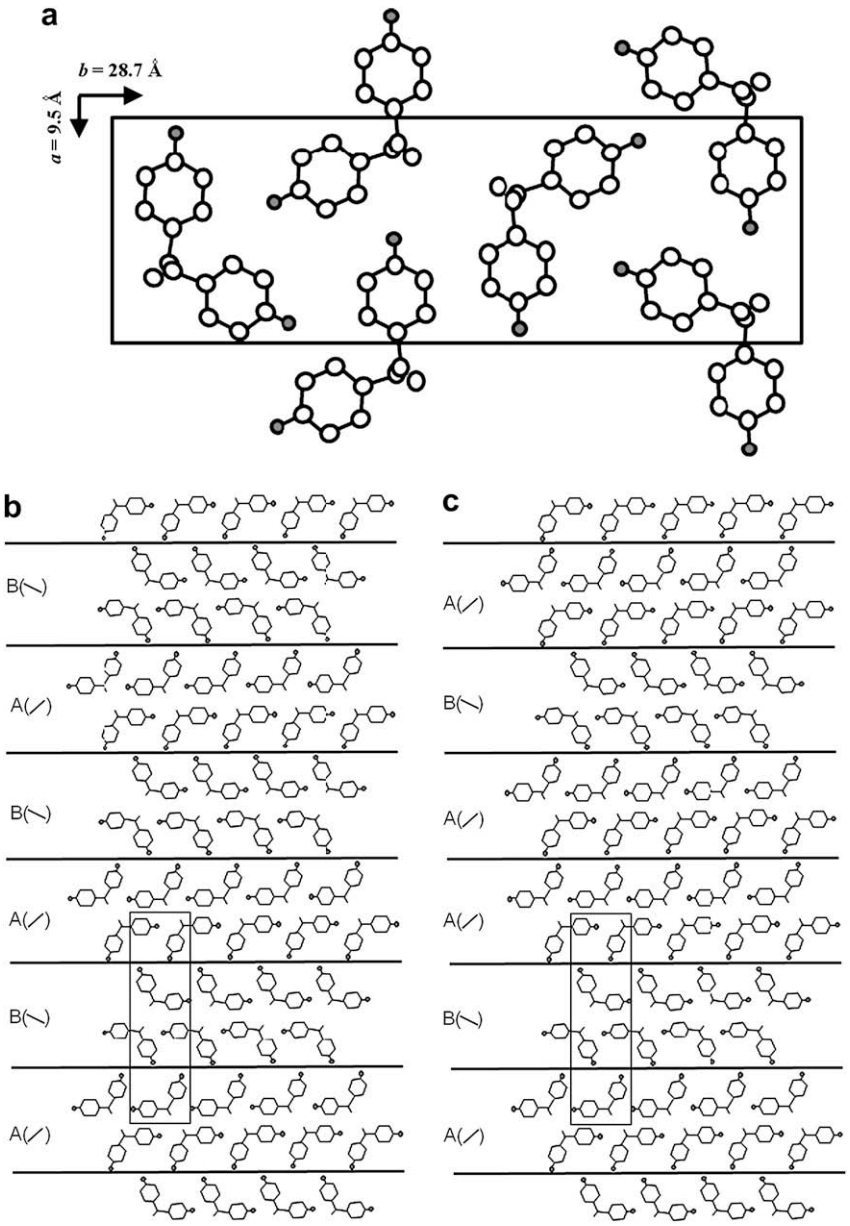

Fig. 7. (a) Schematic presentation of the unit cell of the orthorhombic (β) phase of s-PPFS. (b, c) Possible stacking of polymer bilayers in the crystals. The symbols (/) and (\) indicate the orientations of the lines connecting the adjacent phenyl rings of each chain inside the polymer bilayers A and B, respectively. The regular sequence of bilayers ABABAB… gives rise to the limit ordered β″ modification (b) while a complete disorder in the stacking of these bilayers gives rise to the limit disordered β′ modification (c).

rather similar to the orthorhombic unit cell of the β phase of s-PS ($a = 8.81$ Å, $b = 28.82$ Å, $c = 5.1$ Å) [69,70]. In fact, the only substantial difference is an increase of nearly 8% of the a axis. The Miller indexes of the main reflections have also been indicated close to the curves c and d of Fig. 2.

It is worth noting that the two crystalline peaks appearing as a consequence of high-temperature annealing procedures (indicated by arrows in Fig. 2d) are the only observed peaks characterized by $h + k = 2n + 1$.

The X-ray diffraction patterns of unoriented s-PS samples, exhibiting the β phase, and being in particular close to the limit disordered β′ and limit ordered β″ modifications (with the main peaks labeled by the Miller indexes) [69,70], are shown for comparison in Fig. 6a and b, respectively.

It is immediately apparent the similarity between the pattern and the indexing of the low-temperature annealed sample of s-PPFS of Fig. 2c and those of the β′ modification of s-PS of Fig. 6a, as well as the similarity in the appearance of reflections characterized by $h + k = 2n + 1$ for the high-temperature annealed sample of s-PPFS of Fig. 2d and for the β″ modification of s-PS of Fig. 6b.

As a consequence we suggest, in analogy with s-PS, to name β the thermally stable and orthorhombic phase ($a = 9.5$ Å, $b = 28.7$ Å, $c = 5.1$ Å) of s-PPFS and to name β′ and β″, the corresponding limit disordered and ordered phases.

As well established for s-PS, these experimental observations are consistent with a packing of *trans*-planar chains according to the space group $P2_12_12_1$ (schematically shown in Fig. 7a), for the limit ordered modification (β″), and with a statistical pseudo-centering on the *a*–*b* face of the unit cell (corresponding to the space group *Cmcm*), for the limit disordered modification (β′).

As discussed, in previous reports for s-PS, both ordered and disordered modifications of the β form can be described in terms of

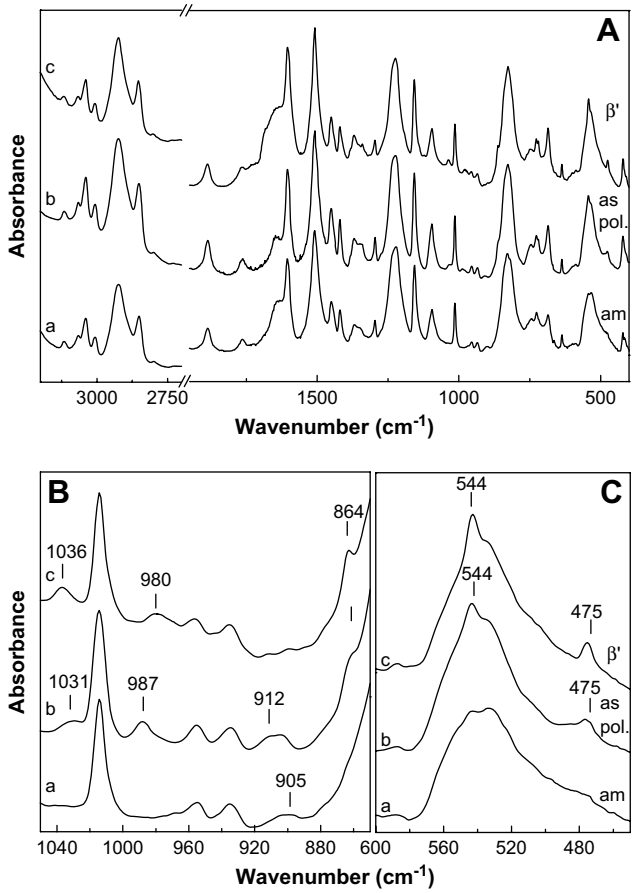

Fig. 8. FTIR spectra of s-PPFS samples: (a) amorphous of Fig. 4a; (b) as-polymerized of Fig. 2a; (c) annealed of Fig. 2c. (A) Spectrum relative to the region 4000–400 cm^{-1}; (B, C) two spectral regions presenting conformational and packing sensitive peaks.

a stacking of the two kinds of *a*–*c* macromolecular bilayers, indicated as A and B in Fig. 7b and c. The limit ordered modification corresponds to a regular alternation of bilayers of type A and B (Fig. 7b) while the limit-disordered modification presents a complete disorder in the stacking of these bilayers (Fig. 7c).

3.4. Infrared spectra

The study of the polymorphic behavior of s-PPFS has allowed obtaining samples completely amorphous or exhibiting the native (possibly co-crystalline) or the β crystalline phases, also controlling the formation of β′ or β″ modifications of the β phase.

This gives the possibility to locate vibrational peaks associated with the ordered conformation that occurs in the crystalline phases. FTIR spectra in the range 4000–400 cm^{-1}, for an amorphous sample and for semicrystalline samples presenting the native and the β′ modification are compared in Fig. 8a–c, respectively. The FTIR spectrum of samples in the β″ modification (not shown) is strictly similar to those of the sample exhibiting the β′ modification.

The spectral regions more sensitive to the conformational order of the polymer chains located in the crystalline phases (1050–800 cm^{-1} and 600–400 cm^{-1}) are shown in detail in Fig. 8B and C, respectively.

Some spectral features are strictly analogous to those observed for s-PS [73–80]. In particular, the semicrystalline samples present, beside the amorphous peak at 905 cm^{-1} (possibly due to out of the plane bending of H atoms belonging to the phenyl groups) [79] a crystalline peak at 912 cm^{-1} (which for s-PS has been attributed to the same vibrational mode [79] and is packing sensitive because for the β phase is observed at 911 cm^{-1} while for the α phase [81,82] is observed at 902 cm^{-1}) [73,77]. It is worth noting that this strict spectral similarity is consistent with the analogous chain packing of the β phases of s-PS and s-PPFS and also suggests that the chain packing of the native crystalline phase of s-PPFS should be somewhat similar to that one of its β phase.

Analogously, the semicrystalline samples, beside the amorphous peak at 833 cm^{-1} (which for s-PS is located 840 cm^{-1} and has also been mainly attributed to the out of plane bending of H atoms belonging to the phenyl groups) [79] present a crystalline peak at 864 cm^{-1} (which for β s-PS is observed at 858 cm^{-1} while for α s-PS is observed at 852 cm^{-1}) [73,77].

It is also worth noting that both amorphous s-PS and s-PPFS present a broad peak at 540 cm^{-1} (which has been attributed to chain modes associated with a ring deformation) [79] while a narrower peak being located at 544 cm^{-1} appears for all crystalline phases of s-PPFS (Fig. 8C) and at 538 cm^{-1} for the *trans*-planar crystalline phases of s-PS [73–76].

These results hence indicate that for s-PPFS not only the orthorhombic phase but also the native (possibly co-crystalline) phase exhibit *trans*-planar polymer chains. In this respect it is worth citing that a co-crystalline phase comprising *trans*-planar chains has been already obtained for s-PPCS in the presence of the *p*-chloro-styrene guest [15].

Particularly relevant to identify by FTIR the two crystalline phases of s-PPFS (native and β) can be the minor peaks that do not appear for the fully amorphous samples, being located at 1031, 987, and 475 cm^{-1} for the native phase and at 1036, 980 and 475 cm^{-1} for the β phase. The absence of analogous "crystalline" peaks for *trans*-planar crystalline phases of s-PS suggests that the vibrational modes also involve the fluoro substituent.

4. Conclusions

Syndiotactic poly(*p*-fluoro-styrene) has been synthesized with improved yields and higher molecular-masses by using a catalytic system based on Cp^*TiCl_3 rather than on $CpTiCl_3$.

The main crystalline phase of s-PPFS, i.e. the only obtained by melt processing or cold-crystallization from the quenched amorphous phase, is orthorhombic ($a = 9.5$ Å, $b = 28.7$ Å, $c = 5.1$ Å). The indexing of the peaks shows a strict analogy with the β orthorhombic phase of s-PS. The similarity also appears more strict in considering the appearance of reflections characterized by $h + k = 2n + 1$, for high-temperature annealing procedures.

In analogy with s-PS, the thermally stable and orthorhombic phase of s-PPFS can be named β and two limit disordered (β′) and ordered (β″) modifications can be defined. The experimental observations are consistent with a packing of *trans*-planar chains according to the space group $P2_12_12_1$, for the limit ordered modification (β″), and with a statistical pseudo-centering on the *a*–*b* face of the unit cell (corresponding to the space group *Cmcm*), for the limit disordered modification (β′), as well established for s-PS.

A different metastable crystalline phase is observed for as-polymerized samples as well as for amorphous samples crystallized by sorption of 1,4-difluoro-benzene. This metastable phase, also after extensive desiccation in vacuum at room temperature, contains substantial amount of residual solvent (3–5 wt%) and is transformed into the orthorhombic phase by annealing as well by any procedure of solvent removal. This suggests that the metastable phase is a co-crystalline phase with the low-molecular-mass guest molecules.

The degree of crystallinity of the s-PPFS samples, independently of the crystallization procedure and also after extensive annealing, remains always lower than 30%. This is consistent with the relatively low syndiotacticity.

DSC scans show the occurrence of a high melting temperature of the orthorhombic phase (321 °C), close to that one observed for s-PPCS (324 °C) and much higher than that one of the analogous orthorhombic s-PS β phase (≈270 °C). As reasonably expected, the T_g of s-PPFS is similar to that one of s-PPMS and intermediate between those of s-PPCS and s-PS.

FTIR spectra have clearly established that for s-PPFS not only the orthorhombic phase but also the native (possibly co-crystalline) phase exhibit *trans*-planar polymer chains. Moreover, FTIR peaks suitable for rapid and easy identification of the two crystalline phases of s-PPFS (native and β) have been reported.

Acknowledgements

The authors thank Dr. Patrizia Oliva, Mariagrazia Napoli and Ivano Immediata of the University of Salerno for useful discussions and experimental support. Financial support of the "Ministero dell'Istruzione, dell'Università e della Ricerca" (PRIN07) and of "Regione Campania" (Centro di Competenza per le Attività Produttive) is gratefully acknowledged.

References

[1] Ishihara N, Seimiya T, Kuramoto M, Uoi M. Macromolecules 1986;19(9):2464–5.
[2] Ishihara N, Kuramoto M, Uoi M. (Idemitsu Kosan Co., Ltd., Japan) EP 210615; 1987; US Patent 5, 502, 133; 1996.
[3] Grassi A, Pellecchia C, Longo P, Zambelli A. Gazz Chim Ital 1987;117(4):249–50.
[4] Ishihara N, Kuramoto M, Uoi M. Macromolecules 1988;21(12):3356–60.
[5] Guerra G, Vitagliano VM, De Rosa C, Petraccone V, Corradini P. Macromolecules 1990;23(5):1539–44.
[6] Corradini P, Guerra G. Adv Polym Sci 1992;100:182–217.
[7] Chatani Y, Shimane Y, Inoue Y, Inagaki T, Ishioka, Ijitsu T, et al. Polymer 1992;33(3):488–92.
[8] Rizzo P, Albunia AR, Guerra G. Polymer 2005;46(23):9549–54.
[9] Rizzo P, D'Aniello C, De Girolamo Del Mauro A, Guerra G. Macromolecules 2007;40(26):9470–4.
[10] Iuliano M, Guerra G, Petraccone V, Corradini P, Pellecchia C. New Polym Mater 1992;3(2):133–44.
[11] De Rosa C, Petraccone V, Guerra G, Manfredi C. Polymer 1996;37(23):5247–53.
[12] Ruiz De Ballesteros O, Auriemma F, De Rosa C, Floridi G, Petraccone V. Polymer 1998;39(15):3523–8.
[13] Esposito G, Tarallo O, Petraccone V. Macromolecules 2006;39(15):5037–42.
[14] Thomann R, Sernetz F, Heinemann J, Steinmann S, Mülhaupt R, Kressler J. Macromolecules 1997;30(26):8401–9.
[15] De Girolamo Del Mauro A, Loffredo F, Venditto V, Longo P, Guerra G. Macromolecules 2003;36(20):7577–84.
[16] De Rosa C, Buono A, Caporaso L, Petraccone V. Macromolecules 2001;34(21):7349–54.
[17] Petraccone V, Tarallo O, Califano V. Macromolecules 2003;36(3):685–91.
[18] Chatani Y, Shimane Y, Inagaki T, Ijitsu T, Yukinari T, Shikuma H. Polymer 1993;34(8):1620–4.
[19] Chatani Y, Shimane Y, Inagaki T, Shikuma H. Polymer 1993;34(23):4841–5.
[20] De Rosa C, Rizzo P, Ruiz de Ballesteros O, Petraccone V, Guerra G. Polymer 1998;40(8):2103–10.
[21] Tarallo O, Petraccone V. Macromol Chem Phys 2004;205(10):1351–60.
[22] van Hooy-Corstjens CSJ, Magusin PCMM, Rastogi S, Lemstra PJ. Macromolecules 2002;35(17):6630–7.
[23] Petraccone V, Tarallo O, Venditto V, Guerra G. Macromolecules 2005;38(16):6965–71.
[24] Tarallo O, Petraccone V, Venditto V, Guerra G. Polymer 2006;47(7):2402–10.
[25] Malik S, Rochas C, Guenet J-M. Macromolecules 2006;39(3):1000–7.
[26] Galdi N, Albunia AR, Oliva L, Guerra G. Macromolecules 2006;39(26):9171–6.
[27] Petraccone V, La Camera D, Pirozzi B, Rizzo P, De Rosa C. Macromolecules 1998;31(17):5830–6.
[28] Petraccone V, La Camera D, Caporaso L, De Rosa C. Macromolecules 2000;33(7):2610–5.
[29] La Camera D, Petraccone V, Artimagnella S, Ruiz de Ballesteros O. Macromolecules 2001;34(22):7762–6.
[30] Loffredo F, Pranzo A, Venditto V, Longo P, Guerra G. Macromol Chem Phys 2003;204(5/6):859–67.
[31] Petraccone V, Esposito G, Tarallo O, Caporaso L. Macromolecules 2005;38(13):5668–74.
[32] Esposito G, Tarallo O, Petraccone V. Eur Polym J 2007;43(4):1278–87.
[33] Tarallo O, Esposito G, Passarelli U, Petraccone V. Macromolecules 2007;40(15):5471–8.
[34] De Rosa C, Guerra G, Petraccone V, Pirozzi B. Macromolecules 1997;30(14):4147–52.
[35] Reverchon E, Guerra G, Venditto V. J Appl Polym Sci 1999;74(8):2077–82.
[36] Milano G, Venditto V, Guerra G, Cavallo L, Ciambelli P, Sannino D. Chem Mater 2001;13(5):1506–11.
[37] Sivakumar M, Mahesh KPO, Yamamoto Y, Yoshimizu H, Tsujita Y. J Polym Sci Part B Polym Phys 2005;43(14):1873–80.
[38] Gowd EB, Shibayama N, Tashiro K. Macromolecules 2006;39(24):8412–8.
[39] Rizzo P, Daniel C, De Girolamo Del Mauro A, Guerra G. Chem Mater 2007;19(16):3864–6.
[40] Petraccone V, Ruiz de Ballesteros O, Tarallo O, Rizzo P, Guerra G. Chem Mater 2008;20(11):3663–8.
[41] Musto P, Manzari M, Guerra G. Macromolecules 1999;32(8):2770–6.
[42] Albunia AR, Graf R, Guerra G, Spiess HW. Macromol Chem Phys 2005;206(7):715–24.
[43] Venditto V, De Girolamo Del Mauro A, Mensitieri G, Milano G, Musto P, Rizzo P, et al. Chem Mater 2006;18(9):2205–10.
[44] Annunziata L, Albunia AR, Venditto V, Mensitieri G, Guerra G. Macromolecules 2006;39(26):9166–70.
[45] Rizzo P, Lamberti M, Albunia AR, Ruiz de Ballesteros O, Guerra G. Macromolecules 2002;35(15):5854–60.
[46] Rizzo P, Costabile A, Guerra G. Macromolecules 2004;37(8):3071–6.
[47] Rizzo P, Spatola A, De Girolamo Del Mauro A, Guerra G. Macromolecules 2005;38(24):10089–94.
[48] Albunia AR, Milano G, Venditto V, Guerra G. J Am Chem Soc 2005;127(38):13114–5.
[49] Albunia AR, Annunziata L, Guerra G. Macromolecules 2008;41(7):2683–8.
[50] Uda Y, Kaneko F, Tanigaki N, Kawaguchi T. Adv Mater 2005;17(15):1846–50.
[51] Venditto V, Milano G, De Girolamo Del Mauro A, Guerra G, Mochizuki J, Itagaki H. Macromolecules 2005;38(9):3696–702.
[52] De Girolamo Del Mauro A, Carotenuto M, Venditto V, Petraccone, Scoponi M, Guerra G. Chem Mater 2007;19(24):6041–6.
[53] Daniel C, Galdi N, Montefusco T, Guerra G. Chem Mater 2007;19(13):3302–8.
[54] Stegmaier P, De Girolamo Del Mauro A, Venditto V, Guerra G. Adv Mater 2005;17(9):1166–8.
[55] D'Aniello C, Musto P, Venditto V, Guerra G. J Mater Chem 2007;17(6):531–5.
[56] Manfredi C, Del Nobile MA, Mensitieri G, Guerra G, Rapacciuolo M. J Polym Sci Part B Polym Phys Ed 1997;35(1):133–40.
[57] Musto P, Mensitieri G, Cotugno S, Guerra G, Venditto V. Macromolecules 2002;35(6):2296–304.
[58] Saitoh A, Amutharani D, Yamamoto Y, Tsujita Y, Yoshimizu H, Okamoto S. Polym J 2003;35(11):868–71.
[59] Daniel C, Alfano D, Venditto V, Cardea S, Reverchon E, Larobina D, et al. Adv Mater 2005;17(12):1515–8.
[60] Malik S, Roizard D, Guenet JM. Macromolecules 2006;39(18):5957–9.
[61] Albunia AR, Minucci T, Guerra G. J Mater Chem 2008;18(9):1046–50.
[62] Daniel C, Sannino D, Guerra G. Chem Mater 2008;20(2):577–82.
[63] Mensitieri G, Venditto V, Guerra G. Sens Actuators B 2003;B92(3):255–61.
[64] Cusano A, Pilla P, Contessa L, Iadicicco A, Campopiano S, Cutolo A, et al. Appl Phys Lett 2005;87(23):234105/1–234105/3.
[65] Giordano M, Russo M, Cusano A, Mensitieri G, Guerra G. Sens Actuators B 2005;109(2):177–84.
[66] Cusano A, Iadicicco A, Pilla P, Contessa L, Campopiano S, Cutolo A, et al. J Lightwave Technol 2006;24(4):1776–86.
[67] Buono A, Rizzo P, Immediata I, Guerra G. J Am Chem Soc 2007;129(36):10992–3.
[68] Guadagno L, Raimondo M, Silvestre C, Immediata I, Rizzo P, Guerra G. J Mater Chem 2008;18(5):567–72.
[69] De Rosa C, Rapacciuolo M, Guerra G, Petraccone V, Corradini P. Polymer 1992;33(7):1423–8.
[70] Chatani Y, Shimane Y, Ijitsu T, Yukinari T. Polymer 1993;34(8):1625–9.
[71] Guerra G, De Rosa C, Vitagliano VM, Petraccone V, Corradini P. J Polym Sci Polym Phys 1991;29(3):265–71.
[72] Guerra G, De Rosa C, Vitagliano VM, Petraccone V, Corradini P, Karasz FE. Polym Commun 1991;32(1):30–2.
[73] Guerra G, Musto P, Karasz FE, MacKnight WJ. Makromol Chem 1990;191(9):2111–9.
[74] Vittoria V. Polym Commun 1990;31(7):263–5.
[75] Kobayashi M, Nakaoki T, Ishihara N. Macromolecules 1989;22(11):4377–82.
[76] Reynolds NM, Hsu SL. Macromolecules 1990;23(14):3463–72.
[77] Musto P, Tavone S, Guerra G, De Rosa C. J Polym Sci Polym Phys 1997;35(7):1055–66.
[78] Yoshioka A, Tashiro K. Macromolecules 2003;36(9):3001–3.
[79] Torres FJ, Civalleri B, Pisani C, Musto P, Albunia AR, Guerra G. J Phys Chem B 2007;111(23):6327–35.
[80] Albunia AR, Rizzo P, Guerra G, Torres FJ, Civalleri B, Zicovich-Wilson CM. Macromolecules 2007;40(11):3895–7.
[81] De Rosa C, Guerra G, Petraccone V, Corradini P. Polym J 1991;23(12):1435–42.
[82] Cartier L, Okihara T, Lotz B. Macromolecules 1998;31(10):3303–10.